HAL
open science

Evaluation of vulcanization nanoactivators with low zinc content: characterization of zinc oxides, cure, physico-mechanical properties, Zn 2+ release in water and cytotoxic effect of EPDM compositions

A. A Gujel, M. Bandeira, C. Menti, D. Perondi, Régis Guégan, M. Roesch-Ely, M. Giovanela, J. S Crespo

To cite this version:

A. A Gujel, M. Bandeira, C. Menti, D. Perondi, Régis Guégan, et al.. Evaluation of vulcanization nanoactivators with low zinc content: characterization of zinc oxides, cure, physico-mechanical properties, Zn 2+ release in water and cytotoxic effect of EPDM compositions. Polymer Engineering and Science, 2018, 58 (10), pp.1800-1809. 10.1002/pen.24781 . insu-01708793

HAL Id: insu-01708793

https://insu.hal.science/insu-01708793v1

Submitted on 8 Jan 2019

HAL is a multi-disciplinary open access archive for the deposit and dissemination of scientific research documents, whether they are published or not. The documents may come from teaching and research institutions in France or abroad, or from public or private research centers.

L'archive ouverte pluridisciplinaire **HAL**, est destinée au dépôt et à la diffusion de documents scientifiques de niveau recherche, publiés ou non, émanant des établissements d'enseignement et de recherche français ou étrangers, des laboratoires publics ou privés.

Evaluation of vulcanization nanoactivators with low zinc content: characterization of zinc oxides, cure, physico-mechanical properties, Zn^{2+} release in water and cytotoxic effect of EPDM compositions

A. A. Gujel[a], M. Bandeira[a], C. Menti[b], D. Perondi[a], R. Guégan[c,*], M. Roesch-Ely[b], M. Giovanela[a] and J. S. Crespo[a,*]

[a]*Universidade de Caxias do Sul, Rua Francisco Getúlio Vargas, 1130, Caxias do Sul, 95070-560, RS, Brazil.*

[b]*Instituto de Biotecnologia, Universidade de Caxias do Sul, Rua Francisco Getúlio Vargas, 1130, Caxias do Sul, 95070-560, RS, Brazil*

[c]*Institut des Sciences de La Terre d'Orléans, UMR 7327, CNRS – Universite d'Orléans, 1A rue de La Férollerie 45071, Orléans Cedex 2, France.*

Phone/Fax: + 55 54 32182159. E-mail: jscrespo@ucs.br and regis.guegan@univ-orleans.fr Phone: + 33 (0)238492541

ABSTRACT

The aim of this work is to evaluate the impact of the reduction of zinc content in Ethylene, Propylene and Diene Monomer (EPDM) elastomeric compositions. Vulcanization nanoactivators ZnO 30 (ZnO dispersed in $CaCO_3$) and ZnO 40 (active ZnO) were used as reinforcers in the elastomers, and both the properties and the cytotoxicity were investigated and compared to those of EPDM with a standard zinc oxide (sZnO) commonly used in the bus rubber profile industry. After a complete description of the physico-chemical characteristics of whole zinc oxides, the vulcanization activators were dispersed in EPDM. Although elastomers with sZnO display a cytotoxic behavior, EPDM formulations containing ZnO 30 and ZnO 40 appeared to be environmental friendly while displaying similar mechanical properties to that with a composition with sZnO. ZnO 30 represents the most interesting vulcanization activator to replace sZnO allowing a reduction of zinc content of 77% without any loss of mechanical properties. Moreover, the formulations associating this nanoactivator show the lowest release of Zn^{2+} in water with a poor cytotoxicity in comparison to sZnO one.

Keywords: EPDM compositions; Nanoactivators; Environmental friendly materials; Cell viability assay

1. Introduction

Ethylene-propylene-diene-monomer (EPDM) plays an important role to both the scientific and technological communities regarding its intensive usage growth in these recent years. However, EPDM requires the addition of vulcanization activators in their formulations for a proper use with the expected properties in commercial applications. Zinc oxide (ZnO) and stearic acid were traditionally used as vulcanization activators in EPDM formulations. These EPDM additives play a dual role as (i) reinforcers improving the processability and the whole physical, mechanical and thermal properties; and (ii) initiators in the sulfur cure of the elastomer [1,2].

As an oligoelement, zinc (Zn) is primordial for numerous ecosystems, however its ecotoxicology at high concentration was frequently reported in the literature. Several studies pointed out a slow growth for several plants with profound toxic effect in the presence of considerable Zn amount [3-5]. Moreover, this element, disrupt various physiological processes and leading in the asphyxiation of some fishes due to mucosal coagulation in their gills.

Among the possible sources of anthropic Zn pollution, the main Zn release in the environment arises from tires and other rubber products. Gope et al. stressed out the close relation between the high amount of zinc in street dust and intense traffic areas [6-9]. If not used or not recycled, reused in other technologies, waste tire wear leacheates still contribute to a pollution with harmful impacts in the envinronement with even toxic effects onto human cells [10,11].

Thus, the current research efforts move towards novel vulcanization activators with a low Zn content in elastomeric compounds [12]. As alternative additives, ZnO with a large specific surface area [1, 13, 14], zinc carboxylates [12,15-17], non-zinc metal oxide

activators, moderate heavy metal activator use, or heavy metal-free activators [18,19] were developed and introduced in EPDM formulations. Although these studies pointed out the benefits in using these materials as alternative vulcanization activators without altering the physico-mechanical properties of EPDM, none or rare research works except one from our group at our knowledge [15] focus on both the toxicity effects and the release of zinc in water.

In that research frame, the purpose of this study concerns the use of two different zinc oxides: ZnO 30 (ZnO dispersed in $CaCO_3$) and ZnO 40 (active ZnO) as low Zn content vulcanization nanoactivators and to characterize their impacts on the mechanical properties, the Zn release in water as well as the cytotoxic effect of EPDM composite leachates.

2. Materials and methods

2.1 Materials

The materials used in this study includ EPDM (Buna EPG 385, Lanxess), carbon black Spheron 5000 (Cabot Corporation), $CaCO_3$ (Carbominer Cargas Minerais), stearic acid (Proquitec Indústria de Produtos Químicos S/A), naphtenic oil 600 N (Agecom Produtos de Petróleo Ltd.), sulfur (Basile Química Indústria e Comércio Ltd.), 1,2-dihydro-2,2,4-polymerized quinoline (TMQ) (Interquímica Comércio e Indústria de Produtos Químicos Ltd.), N-cyclohexyl-2-benzothiazole sulfonamide (CBS) (Interquímica Comércio e Indústria de Produtos Químicos Ltd.), and tetramethylthiuram disulphide (TMTD) (Interquímica Comércio e Indústria de Produtos Químicos Ltd.).

For the development of different elastomeric compositions, a standard ZnO (named sZnO, Votorantin) and two nano ZnO (active ZnO, named ZnO 40 from Global

Chemical CO., Ltd., and ZnO dispersed in $CaCO_3$, named ZnO 30 from Global Chemical CO., Ltd.) were used.

For the cytotoxic tests the following materials were used: human lung fibroblast obtained from American Type Culture collection (ATCC), cell medium Dulbecco´s Modified Eagle's Medium (DMEM, Sigma-Aldrich), fetal bovine serum (FBS, Sigma-Aldrich), penicillin-streptomycin (Gibco-BRL), (3-(4,5-dimethylthiazol-2-yl)-2,5-diphenyltetrazolium bromide) (MTT, Sigma-Aldrich) and dimethyl sulfoxide (DMSO, Sigma-Aldrich).

2.2 Characterization of zinc oxides

2.2.1 Atomic absorption spectrometry (AAS)

The zinc content in the sZnO, ZnO 30 and ZnO 40 samples was determined using a Perkin Elmer Analyst 200 spectrometer after preliminary acid digestion of the vulcanization activators with a solution of HNO_3 (10% v/v).

2.2.2 X-ray diffraction analysis (XRD)

XRD patterns of sZnO, ZnO 30 and ZnO 40 samples were recorded in a Thermo Electron ARL'XTRA diffractometer equipped with a Cu anode and a Si(Li) solid detector. A counting time of 20 sper 0.02°2θ step was used as the experimental measurement parameter. The divergence, incident beam scatter, diffracted beam scatter and receiving slit width were 1.00, 1.50, 0.45 and 0.30 mm, respectively.

2.2.3 Analysis of specific surface area and pore distribution

About100 mg of each vulcanization activator were degassed at 383 K for 24 h at a pressure of 0.01 Pa. The measurements were performed at 77 K using a NOVA Surface Analyzer (Quantachrome Instruments). Data were recorded for relative vapor pressures from 0.05 to 0.99. The specific surface area was determined using the Brunauer-Emmet-Teller (BET) equation based upon the cross-sectional area of nitrogen at 77 K. Pore size distributions were calculated using the NOVAWin software according to the Barret, Joyner and Halenda (BJH) method and with the density functional theory method.

2.2.4 Particle size characterization

The particle size distribution of sZnO, ZnO 30 and ZnO 40 samples was determined using a Horiba particle size distribution analyzer LA-950. The tests were performed in triplicate.

2.2.5 Morphological study (FESEM)

The morphology and particle size of sZnO, ZnO 30 and ZnO 40 samples were examined by field emission scanning electron microscopy (FESEM) performed by a Tescan MIRA 3 apparatus equipped with an energy beam of 15 kV.

2.3 Preparation of elastomeric compositions

The elastomeric compositions were prepared based on a standard composition for bus body rubber profiles with the following proportions in parts per hundred of rubber (phr): EPDM (100), ZnO (1, 2, 3, 4 and 5), stearic acid (1.5), carbon black (75), naphthenic oil (25), $CaCO_3$ (30), TMQ (2), sulfur (1.8), CBS (1.5), and TMTD (1). The

sZnO was replaced by ZnO 30 and ZnO 40 in the same proportion. A sample without ZnO (0 phr) was also prepared and analyzed for comparative purposes.

These elastomeric compositions were prepared using industrial two-roll mill(Luxor) with rollers of 300 × 700 mm and capacity of 15 kg. The addition of the additives consisted of the elastomer, fillers, oil, acid stearic, TMQ, sulfur, CBS and TMTD.

The incorporation of sZnO, ZnO 30 and ZnO 40 were carried out using a laboratory two-roll mill (*homemade*) with capacity of 500 g at 60°C.

2.4 Characterization of elastomeric compositions

2.4.1 Mooney viscosity

Viscosity characteristics were determined in a MV-2000 Mooney viscometer from Alpha Technologies Inc. (Bellingham) using a large rotor at 100°C for 5 min with 1 min of preheating, according to ASTM: D1646.

2.4.2 Cure characteristics

Curing characteristics were determined using a MDR 2000 oscillating disk rheometer from Alpha Technologies Inc. (Bellingham) 160°C, according to ASTM: D2084.

2.4.3 Morphological study (FESEM)

The morphology of the compositions sZnO 4 phr, ZnO 30 3 phr and ZnO 40 2 phr were obtained by field emission scanning electron microscopy (FESEM) performed by a Tescan MIRA 3 apparatus equipped with an energy beam of 5 kV.

2.4.4 Cross-link density

The cross-link density [*X*] was obtained by measuring swelling using the Flory-Rehner equation [18] with the Kraus correction [20,21] (Equation 1):

$$[X] = \frac{-\left[\ln(1-\upsilon_r) + \upsilon_r + \chi \cdot \upsilon_r^2\right]}{V_o\left(\upsilon_r^{1/3} - \upsilon_r/2\right)} \text{ (Eq. 1)}$$

whereυ_r is the volume fraction of swollen rubber, χ is the polymer-solvent interaction parameter (0.35)and V_o is the molar volume of solvent (147.47 cm^3 mol^{-1}) [21].

Samples with dimensions of 20 × 20 × 2 mm were immersed in heptane in the dark at 23 ± 2°C for 72 h, and then immediately weighed to measure their weights when swollen. Subsequently, the samples were dried at 60°C under vacuum for 12 h, and weighed again to find the dry weights after swelling.

2.4.5 Physico-mechanical characterization

The specimens of the samples were obtained by compression molding at 160°C under a pressure of 7.5 MPa in a Shultz electrically heated hydraulic press (Shultz S/A) forthe optimum cure time (t_{90}), according to ASTM: D2640.

A Shore AGS709 Teclock durometer (Japan) was used to measure hardness according to ASTM: D2240. Tensile and tear strength tests were performed in an EMIC DL-3000 instrument (Intron Equipamentos Científicos Ldt.) according to ASTM: D412 and ASTM: D624, respectively. The density was determined according to ASTM:

D297.All these tests were performed after 40 h of conditioning at 23 ± 2°C and a relative humidity of 50 ± 5%.

2.4.6 Analysis of zinc release in water

Approximately 10 g of each elastomeric composition with the same content of Zn^{2+}(sZnO 4phr, ZnO 30 3 phr and ZnO 40 2 phr)in pieces of 0.5 cm^2 were placed in 100 mL of distilled water under continuous stirring in an orbital shaker. Water samples were taken at 30, 60, 90, 120, 240 and 360 min. At the end of this procedure, the water samples were analyzed byAAS to quantify the zinc content.

2.5 Cytotoxic effect of elastomeric compositions

2.5.1 Extraction conditions

About 10 g of each elastomeric composition in pieces of 0.5 cm^2 with the same content of Zn^{2+}(sZnO 4 phr, ZnO 30 3 phr and ZnO 40 2 phr) were placed in 100 mL of DMEM. Samples were placed in 37°C chamber under continuous stirring in orbital shaker (65 rpm), and were taken at 30, 60, 90, 120, 240 and 360 min after extraction. Extraction conditions followed standard protocols taken from ISO 10993−12:2004. Samples were kept at 4°C until cell exposition.

2.5.2 Cell viability assay

MRC5 cell line was purchased from the ATCC. Cells were cultured in DMEM, supplemented with 10% of FBS and 1% of penicillin-streptomycin. MRC-5 was kept in a humidified atmosphere at 37ºC and 5% of CO_2.

Briefly, 1.0 $\times 10^5$ cells were inoculated for analysis until 80% of confluence was reached. Treatment with different elastomers and isolated compounds was performed, according to subitems “a” and “b” from this section. After treatment, cell cytotoxicity was assessed through 3-(4,5-dimethylthiazol-2-yl)-2,5-diphenyltetrazolium bromide (MTT), an indirect cytotoxic test based on the formation and colorimetric quantification of an enzyme reaction product (formazan), which evaluates the reduction of the MMT.

MTT solution (1.0 mg mL^{-1} in serum-free medium) was added for 2 h. The formazan was previously dissolved in dimethyl sulfoxide for 30 min, and the absorbance at 570 nm was measured using a microplate reader (Spectra Max M2e, Molecular Devices).

The quantity of formazan produced is indicative of the number of viable cells in culture. The absorbance of the negative control represents 100%. Control sample refers to exclusive DMEM cell exposition. The percentage of growth inhibition was calculated as: cell viability (%) = (absorbance of experimental wells/absorbance control wells) × 100. Each experiment was performed at least in triplicate.

a) Cell exposure to extracts taken from elastomeric compositions (sZnO 4 phr, ZnO 30 3 phr and ZnO 40 2 phr)

After confluence, MRC-5 cell were incubated with 100 µL of DMEM extracts exposed previously to elastomers. All elastomer were exposed to DMEM and extracts were tested at 30, 60, 90, 120, 240 and 360 min and were incubated for 24 h in a humidified atmosphere at 37ºC and 5% of CO_2, seeded with 10% FBS.

b) Cell exposure to isolated compounds (sZnO, ZnO30, ZnO40 and TMTD)

Once confluence was reached, MRC-5 cell line was exposed to different concentrations of DMEM soluble rubber additives sZnO, ZnO30, ZnO40 and TMTD for 24h incubation.A range of concentration for each compound was tested (2.5, 4.5, 5.0, 10.0, 12.0, 15.0, and 20.0 μg mL^{-1}).

3 Results and discussion

3.1 Characterization of zinc oxides

3.1.1 Atomic absorption spectrometry (AAS)

AAS represents a simple and easy technique for the determination of amount of zinc in sZnO, ZnO 30 and ZnO 40 activators, which reaches 32.8, 43.8 and 69.1 wt% of zinc in their composition, respectively.

3.1.2 X-Ray diffraction analysis (XRD)

Fig. 1 shows the XRD patterns of the whole vulcanization nanoactivators: ZnO 30 (ZnO dispersed in $CaCO_3$) and ZnO 40 (active ZnO), and sZnO. sZnO displays diffraction peaks characteristics of calcite [24], dolomite [25] and zincite [26] mineral phases. Since ZnO is a sample of industrial use, it is not a surprise that this material contains impurities from the manufacturing process or its mineral source.

Both ZnO 30 and ZnO 40 display diffraction peaks characteristics of zincite [26], at the angular values of 31.8º, 34.6º and 36.2º. The width at half maximum of these diffracted peaks is somehow broader than the sZnO, underlining here a difference in the size of coherent domains for the diffraction with small particles or low crystalline samples. Based on the hypothesis that sZnO contains well crystalline zincite with a percentage of crystallinity reaching 95%, the crystallinity of ZnO 30 was estimated to 34% whereas that

of ZnO 40 approached 82% [1]. Other mineral phases complete the X-ray diffraction patterns of two alternative activators such as wurtzite [27], a mineral with a compact hexagonal type crystal structure characteristic of ZnO [1]. Since ZnO 30 is mixed with calcite, diffraction peaks characteristics of calcite crystalline phase could be oberserved in the diffractogram [24].

3.1.3 Analysis of specific surface area and pore distribution

The adsorption and desorption isotherms of nitrogen gas for sZnO, ZnO 30 and ZnO 40 samples are shown in **Fig. 2**. According to IUPAC, these isotherms can be classified as type IV [28]. The initial part of the isotherm is attributed to the monolayer-multilayer adsorption since it follows the same path as the corresponding part of a type II isotherm obtained with the given adsorptive on the same surface area of the adsorbent in a nonporous form. The type IV isotherms exhibit hysteresis loops, which are associated with capillary condensation taking place in the mesopores, and a limiting uptake over a range of high P/P_o [28]. The profile of this isotherm is characteristic of mesoporous adsorbents (with pore diameters between 2 and 50 nm) [28,29]. Furthermore, this isotherm shows H4 hysteresis loopsgenerally associated with a wide range of narrow slit-like nanopores [28].

The BET calculation applied to the nitrogen desorption isotherm gave a total specific surface area of 3.44, 16.23 and 23.85 m^2 g^{-1} for sZnO, ZnO 30 and ZnO 40, respectively (Table 1). It is important to remind that the samples are inhomogeneous in their composition of zinc and their mineral phases and it is rather hard to relate their BET specific surface areas with only zincite. Here, the specific surface area is much more correlated to the size of the particles of the whole mineral phases in the samples. X-ray

diffraction patterns revealed the poor crystallinity and size of the ZnO particles for both ZnO 30 and 40 leading to a much rlarge specific surface area than that of sZnO. Interestingly, the whole materials show a d_{pore} intermediate between the threshold values of 2 and 50 nm indicating that vulcanization activators are mesoporous [28].

3.1.4 Aggregates size characterization

The particle size characterization showed that sZnO, ZnO 30 and ZnO 40 samples are composed of aggregates with mean diameters of 13.45±1.49, 4.47±0.25 and 4.29±0.19 μm, respectively. These results indicate that the physically observable smaller particles, also known as primary particles, have high surface forces. As a result, thousands of these particles agglomerate to form so-called secondary particles (aggregates).

ZnO 30 and ZnO 40 built up less aggregates than sZnO, due probably to the impurities content or the low density of ZnO, and size of the particles. This latter observation represents an important point for a uniform dispersion in polymer, i.e., absence of any phase segregation that may favor the reactivity of the vulcanization reaction.

3.1.5 Morphological study (FESEM)

Fig. 3 shows the FESEM images for sZnO, ZnO 30 and ZnO 40 samples.As shown in **Fig. 3(a-c)**, the particles have hexagonal morphology with some spherical structures [29]. However, the sZnO sample (**Fig. 3a**) exhibited agglomeration of hexagonal nanoparticles, which results in the formation of agglomerated ZnO units in the range of 15-20 μm, as observed from the results of analysis of distribution of particle size.

The diameter of the particle of sZnO sample (**Fig. 3a**) spread out from 0.04 to 0.20 μm with a mean average size of approximately 0.080 μm. Taken together with the results of Table 1, the specific surface area of the sZnO suggests that it is classified as a conventional ZnO [14,30].

In **Fig. 3(b-c)**, it was possible to verify the formation of ZnO aggregates with average sizes between 4 and 5 μm, which is in agreement with the results previously obtained by particle size distribution. ZnO 30 and ZnO 40 have average particle sizes of 0.029 and 0.022 μm, respectively (**Fig. 3(b-c)**). Taking into account the results for the specific surface area of ZnO 30 and ZnO 40, these zinc oxides are classified as nano ZnO [14,30].

3.2 Characterization of elastomeric compositions

3.2.1 Mooney viscosity

Table 2 shows the results of Mooney viscosity for the elastomeric compositions. It was observed that the Mooney viscosity values for the compositions with sZnO presented similar results, except the 5 phr sample. For the compositions with ZnO 30 and ZnO 40, there was little variation between 2-5 phr levels, with the exception of 1 phr which had lower Mooney viscosity values.

The sZnO in amounts equivalent to 5 phr serves as a loading filler, thereby influencing viscosity. In contrast, this effect ofthe ZnO 30 and ZnO 40 occurs from the use of amounts equivalent to 2 phr.

3.2.2 Curing properties

The curing characteristics of the elastomeric are shown in Table 3.The M_L results were similar to those of the standard composition, indicating little variation in viscosity and processability. The M_H values,which are related to the molecular rigidity [30], decreased with decreasing ZnO content in all compositions.

For the compositions with ZnO 30 and ZnO 40, these values were higher than those observed for the compositions with sZnO. This result can be justified by the increased specific surface area of ZnO 30 and ZnO 40, making them more reactive. The delta torque values (ΔM) can be used as an indirect indication of the cross-linking density of the elastomeric compounds [32]. These values increased with the increasing ZnO, ZnO 30 and ZnO 40 content. The ΔM values for ZnO 40 were greater than other compositions because it is a more reactive activator and most likely forms of a higher number of cross-links.

The t_{s1} did not change significantly in the compositions with ZnO 30 and ZnO 40, but the values decreased when compared to the composition with sZnO. The t_{90} value decreased in the compositions with higher content of sZnO. This behavior agreed well with the higher CRI values. Moreover, the addition of ZnO 30 and ZnO 40 instead of sZnO seems to accelerate the cure reaction of EPDM system as it incresead the CRI values due to the lower values of t_{s1} and t_{90} for the ZnO 30 and ZnO 40 formulations in comparison with the sZnO compositions.

The vulcanization process of elastomers is divided into two steps: the first step involves a reaction of ZnO particles with the accelerator and sulfur form activated sulfurating species, followed by the reaction of these reactive moieties with the unsaturation sites of rubber chains to form crosslink precursors [33]. The scheme of vulcanization reaction is shown in **Fig. 4**, which is further discussed in the item 3.2.7

based on the cellular viability results. During the first step, ZnO 30 and ZnO 40 have smaller particle sizes compared to sZnO; thus, ZnO 30 and ZnO 40 could penetrate easily into the elastomer matrix and react like polar pathway with the co-activator, acelerator and sulfur molecules embedded between the EPDM chains [1,34-37]. On the other hand, the samples without ZnO and with sZnO reacts mainly through a radical pathway due to the difficulty of dispersion of sZnO particles in the rubber matrix [34,38,39]. Additionally, ZnO 30 and ZnO 40 increases the amount of sulfur absorbed on the activator specific surface area and accelerates the crosslink formation reactions in the second stage of cure process.

These results could be of interest to the rubber industry because the lower t_{90} value and higher CRI value would create lower production costs for rubber goods [40].

3.2.3 Morphological Study

Fig. 5 illustrates the fractured surface of the three compositions developed with the same content of zinc (sZnO 40, ZnO 30 and ZnO 40). The FESEM images shows a rough fracture without the presence of cristal forms in all samples. It can be observed the presence of ZnO esferic evenly distributed in all three compositions. There are also the presence of agglomerates which can be related to $CaCO_3$ or ZnO.

3.2.4 Cross-link density

Fig. 6 shows the cross-link density of the elastomeric compositions.In general, the cross-link density results for the developed compositions increased with increasing ZnO content, especially for compositions with ZnO 30 and ZnO 40, corroborating the M_H and ΔM values. The results for ZnO 30 and ZnO 40 were higher than sZnO. These materials

have a greater specific surface area,which makes them more reactive and promotes more crosslinked networks.

3.2.5 Physico-mechanical characterization

Table 4 shows the hardness and tear strength data for the elastomeric compositions.The hardness values for ZnO 30 and ZnO 40 compositions with 2-5 phr do not change significantly. For compositions with 1 phr, hardness is reduced and can be attributed to a small amount of the activator and the decrease in the crosslink density as noted in **Fig. 7**. For the compositions with sZnO, the reduction of this activator indicated that hardness has been similarly affected. For the composition without ZnO, by other hand, hardness values decreased dramatically, confirming the importance of ZnO as a vulcanization activator in elastomeric formulations.

The elastomeric compositions with sZnO, ZnO 30 and ZnO 40, especially with1 phr, showed greater tear strength results than the other ZnO contents. This can be explained by the decrease in cross-link density in these compounds (**Fig. 6**). It is known that tear strength is enhancedwith small increases in cross-link density up to a limit. The tear strength then decreases with additional cross-linking [41,42]. Heideman et al.[30]have reported that the equivalent replacement for conventional ZnO for nano ZnO leads to an improvement in rubber compound properties. For this reason, the nano ZnO can greatly reduce the ZnO content in elastomeric compounds.

Fig. 7(a-c) shows the tensile strength, modulus at 100% and elongation at break results for the elastomeric compositions with sZnO, ZnO 30 and ZnO 40, respectively.

With the incorporation of 1 to 5 phr of sZnO (**Fig. 7a**), the tensile strength showed similar values. On the other hand, the composition without ZnO showed a decrease in this property,which may be a result ofless cross-linking formation.

For the elongation at break, with the reduction of sZnO content, the values showed an increase that can be attributed to a decrease in the molecular rigidity of the compositions. This was confirmed by the modulus values at 100%. The modulus at 100% decreased with the reduction of sZnO content. This result is interesting because lower values for modulus at 100% are best for installation of profiles on buses [43].

As shown in **Fig. 7b** and **7c,**the properties of tensile strength, elongation at break and modulus at 100% remained constant for ZnO contents from 2 to 5 phr. The only exception was the composition with 1 phr of ZnO 30 and ZnO 40, which showed a decrease in tensile strength and modulus at 100%, while the elongation at break showed an increased. As discussed earlier, these results are due to the decreased cross-link density and rigidity of the matrix when this content of ZnO 30 and ZnO 40 wereused.

3.2.6 Analysis of zinc release in water

The release of zinc in water (%wt of total Zn^{2+}mass) for the elastomeric compositions is shown in **Fig. 8**. There was a Zn^{2+} release in water of less than 1.0% for all samples (sZnO = 2.86 ±0.24 mg L^{-1}; ZnO 30 = 1.86 ±0.52 mg L^{-1}; ZnO 40 =2.07 ±0.33 mg L^{-1}). Similar results were observed by Moresco et al. in NR passenger tire tread compositions [15]. The ZnO 30 and ZnO 40 released less Zn^{2+} into the aqueous environment.

These nanoactive zinc oxides have greater specific surface area than the sZnO and most of the free Zn^{+2} formed organic complexes with accelerators (**Fig. 4** – polar

pathway). Thus, ZnO30 and ZnO 40 are the most efficient for the vulcanization process, with increased crosslink network chain formation (**Fig. 6**). For ZnO 30, the zinc release was the lowest of other zinc oxides, indicating that the product is themost environmentally friendly material.

3.2.7. Cell viability after elastomeric compositions exposition

The cell viability of the leachates from the elastomeric composition was evaluated and the results are show in **Fig. 9**.

After 24h incubation of extracts exposed to different elastomers, no cytotoxic effectswere observed in the ZnO 30 and ZnO 40 samples along all extraction times. However, a reduction on cell viability exposed to extraction at 90 min of the sample without ZnO was observed, with a progressive cytotoxic effect once extraction time increased. The elastomeric composition with sZnO presented an expressive cytotoxic profile with incubation of extracts left for 60 min in contact with DMEM medium.

In order to evaluate the effects of isolated compounds on cell viability, MRC-5 was exposed to different concentrations of DMEM soluble additives sZnO, ZnO 30, ZnO 40 and TMTD for 24 h. The results are shown in **Fig. 9**. A range of concentration for each compound was tested (2.5 - 20.0 μg mL^{-1}). While ZnO30 and ZnO40 presented a similar cytotoxic profile, cell viability decreased only after high exposition concentration (15.0 μg mL^{-1}), MRC-5 was more susceptible to sZnO, with decrease in cell viability from 10.0 μg/mL. In an interesting perspective, a considerable cytotoxic effect was rapidly observed in cells after exposition to minimum doses of TMTD (2.0 μg mL^{-1}).

The TMTD concentration in the elastomeric compositions may reach a value of 410 μg mL^{-1}. According to **Fig. 4**, the samples without ZnO and with sZnO react mainly

by radical pathway where the TMTD is used as a catalyser and becomes a byproduct in the end of the reaction. The extraction of the TMTD formed in the radical vulcanization reaction can explain the cytotoxic effect observed in the samples without ZnO and with sZnO. The samples with ZnO 30 and ZnO 40 have a polar vulcanization reaction, thus consuming all TMTD present, leaving no cytotoxic byproduct at the end of the reaction.

Since the Zn^{2+}-free composition (sample without ZnO) showed a toxic effect and considering that the concentration of zinc released by the compositions with sZnO (0.25 μg mL^{-1}), ZnO 30 (0.14 μg mL^{-1}) and ZnO 40 (0.20 μg mL^{-1}) is lower than the value considered as toxic (**Fig. 10**), it is likely that the zinc released by the compositions is not associated with the cytotoxic effect here observed.

4. Conclusions

The use of vulcanization nanoactivators was compelling because similar results were obtained with lower levels of ZnO, from 5 phr of sZnO to 2 phr ZnO 30 (77% reduction in zinc content) and 5 phr of sZnO to 2 phr of ZnO 40 (62% reduction in zinc content), without impacting the properties of the elastomeric compositions. The elastomeric compositions with 2 phr of ZnO 30 showed the lowest Zn^{2+} release in water and are thus the most environmentally friendly.

Given the significant contribution of tire particles to ambient and that traffic exposure has been significantly associated with adverse health effects, further cytotoxic study is mandatory. The findings suggest that, the cytotoxic effect was subordinate to conditions of manufacture product release. The samples with ZnO 30 and ZnO 40 have a polar vulcanization reaction, thus consuming all TMTD present and forming no cytotoxic byproduct, leading to a less aggressive cytotoxic product. The consequences of a residual

toxic product to environment are of great impact and further investigations of potential toxicity of products leached by rubber materials on water biota should be investigated.

Cell signals to different aggressive stimuli, which are dependent mostly on toxin concentration and time of exposition, among others. Changes in the way products are process generates a huge variety of toxic effects to cells. As observed in this study, although sZnO samples were toxic to cells, no cytotoxic effects were observed in the elastomeric compositions with ZnO 30 and ZnO 40.

5. Acknowledgements

The authors are grateful to Ciaflex Rubber Industry Ltda., Auriquímica Ltd., PCR Artefatos de Borracha, FAPERGS (11/33650-0) and FINEP (01.13.0359-00).

6. References

[1] S. Akhlaghi, M. Kalaee, S. Mazinani, E. Jowdar, A. Nouri, A. Sharif, and N. Sedaghat, *Thermochim. Acta*, **527**, 91 (2012).

[2] A. Moezzi, A.M. Mcdonagh, and M.B.Cortie, *Chem. Eng. J.*, **185**, 1 (2012).

[3] I. Alkorta, J. Hernández-allica, J.M. Becerril, I. Amezaga, I. Albizu, and C. Garbisu, *Rev. Environ. Sci. Biotechnol.*, **3**, 71, (2004).

[4] S.M. Nelson, G. Mueller, and D.C. Hemphill, *Environm. Contam. Toxicol.*, **52**, 574, (1994).

[5] J.J. Evans, *Environm. Contam. Toxicol.*, **151**, 64, (1997).

[6] M. Gualtieri, M. Andrioletti, C. Vismara, M. Milani, and M. Camatini, *Environ. Int.*, **31**, 723, (2005).

[7] M. Gope, R. E. Masto, J. George, R. R. Hoque, S. Balachandran, *Ecotoxicology and Environmental Safety*, **138**, 234, (2017).

[8] M. Gualtieri, M. Andrioletti, P. Mantecca, C. Vismara, and M. Camatini, *Particle Fibre Toxicol.*, **2**, 1, (2005).

[9] P. Mantecca, G. Sancini, E. Moschini, F. Farina, M. Gualtieri, A. Rohr, G. Miserocchi, P. Palestini, and M. Camatini, *Toxicol. Lett.*, **189**, 206, (2009).

[10] M. Gualtieri, L. Rigamonti, V. Galeotti, and M. Camatini, *Toxicol. In Vitro*, **19**, 1001, (2005).

[11] E. Beretta, M. Gualtieri, L. Botto, P. Palestini, G. Miserocchi, and M. Camatini, *Toxicol. Lett.*, **173**, 191, (2007).

[12] F.M. Helaly, S.H.E. Sabbagh, O.S.E. Kinawy, and S.M. Sawy, *Mater. Des.*, **32**, 2835, (2011).

[13] B. Panampilly and S. Thomas, *Polymer Engineering and Science*, **56**, 1337, (2013)

[14] N. Vatansever and S. Polat, *Mater. Des.*, **31**, 1533, (2010).

[15] S. Moresco, M. Giovanela, L.N. Carli, and J.S. Crespo, *J. Cleaner Prod.*, **117**, 199, (2016).

[16] A.A. Gujel, M. Bandeira, M. Giovanela, L.N. Carli, R.N. Brandalise, and J.S. Crespo, *Mater. Des.*, **53**, 1119, (2014).

[17] A.A. Gujel, M. Bandeira, V.D. Veiga, M. Giovanela, L.N. Carli, R.S. Mauler, R.N. Brandalise, and J.S. Crespo, *Mater. Des.*, **53**, 1112, (2014).

[18] G. Heideman, J.W.M. Noordermeer, R.N. Datta, and B.V. Baarle, *Macromol. Symp.*, **1**, 657, (2006).

[19] L. Pysklo, P. Pawlovski, and W. Parasiewicz, *KGK Kaut. GummiKunst.*, **60**, 548, (2007).

[20] P.J. Flory, *Principles of Polymer Chemistry*, Cornel University, New York (1953).

[21] G.J. Kraus, *J. Appl. Polym. Sci.*, **7**, 861, (1963).

[22] E. Bilgili, H. Arastoopour, and B. Bernstein, *Powder Technol.*, **115**, 277, (2001).

[23] J.E. Mark, *Polymer Data Handbook*, Oxford University Press, New York (1999).

[24] H. Sowa and H. Ahsbahs, J. *Appl. Crystallog.*, **39**, 169, (2006).

[25] T. Pilati, F. Demartin, and C.M. Gramaccioli, *Acta Crystallog. Sect. B: Struct. Sci.*, **54**, 515, (1998).

[26] V.A. Drits, D.K. Mccarty, B. Sakharov, and K.L. Miliken, *Can. Mineral.*, **43**, 1255, (2005).

[27] G.Y. Chao and R.A. Gault, *Can. Mineral.*, **36**, 775, (1998).

[28] K.S.W. Sing, D.H. Everett, R.A.W. Haul, L. Moscou, R.A. Pierotti, J. Rouquérol, and T. Siemienisewska, *Pure Appl. Chem.*, **57**, 603, (1985).

[29] M. Pudukudy and Z. Yaakob, *Appl. Surf. Sci.*, **292**, 520, (2014).

[30] G. Heideman, R.N. Datta, W.M. Noordermeer, and B. Baarle, *J. Appl. Polym. Sci.*, **95**, 1388, (2005).

[31] M. Balasubramanian, *J. Polym. Res.*, **16**, 133, (2009).

[32] V. Jovanovic, S.S. Jovanovic,J.B. Simendic, G. Markovic, and M.M. Cincovic, *Composites Part B*, **45**, 333, (2013).

[33] M.V. Duin, R. Orza, R. Peters, and V. Chechik, *Macromol. Symp.*, **291**, 66, (2010).

[34] W. Scheele and A. Franck, *Rubber Chem. Technol.*, **38**, 139, (1959).

[35] V. Duchacek, *J. Appl. Polym. Sci.*, **22**, 227, (1978).

[36] V. Duchacek, *J. Appl. Polym. Sci.*, **23**, 2065, (1979).

[37] A. M. Joseph, B. George, K.N. Madhusoodanan, and R. Alex, *Rubber Sci.*, **28**, 82, (2015).

[38] B.A. Dogadkin and V.A. Shershnev, *Rubber. Chem. Technol.*, **33**, 401, (1960).

[39] M.M. Coleman, J.R. Shelton, and J.L. Koenig, *Rubber Chem. Technol.*, **46**, 957, (1973).

[40] A. Zanchet, N. Dal'Acqua, T. Weber, J.S. Crespo, R.N. Brandalise, and R.C.R. Nunes, *Polim.: Cienc. Tecnol.*, **17**, 23, (2007).

[41] A.Y. Coran, *Vulcanization*. In: J.E. Mark, B. Erman, and F.R. Eirich (Eds), Science and Technology of Rubber, Academic Press, New York (1994).

[42] M.R. Krejsa and J.L. Koenig, *Rubber Chem. Technol.*, **66**, 376, (1993).

[43] A. Zanchet, L.N. Carli, M. Giovanela, R.N. Brandalise, and J.S. Crespo, *Mater. Des.*, 39, 437, (2012).

Figure Captions

Figure 1. XRD patterns of sZnO, ZnO 30 and ZnO 40 samples.

Figure 2. Nitrogen gas adsorption/desorption isotherms for sZnO, ZnO 30 and ZnO 40 samples.

Figure 3. FESEM images for **(a)** sZnO, **(b)** ZnO 30 and **(c)** ZnO 40.

Figure 4. Scheme of vulcanization reactions of the samples without ZnO, and with sZnO, ZnO 30 and ZnO 40.

Figure 5. FESEM images of the compositions sZnO 40 4 phr (a), ZnO 30 3 phr (b) and ZnO 40 2 phr (c).

Figure 6. Cross-link density of elastomeric compositions.

Figure 7. Tensile strength, modulus at 100% and elongation at break for the elastomeric compositions with **(a)** sZnO, **(b)** ZnO 30 and **(c)** ZnO 40.

Figure 8. Zn^{2+} release of the elastomeric compositions with sZnO, ZnO 30 and ZnO 40 in water.

Figure 9 . Effect on MRC-5 cell line viability after being in contact to different elastomers after 30, 60, 90, 120, 240 and 360 min. Values are expressed in means ± SD. Dash line control sample refers to exclusive medium (DMEM) cell exposition.

Figure 10. Effect on MRC-5 cell line viability exposed to different concentrations (2.5-20.0 μg mL^{-1}) of sZnO, ZnO 30, ZnO 40 and TMTD after 24 h incubation.

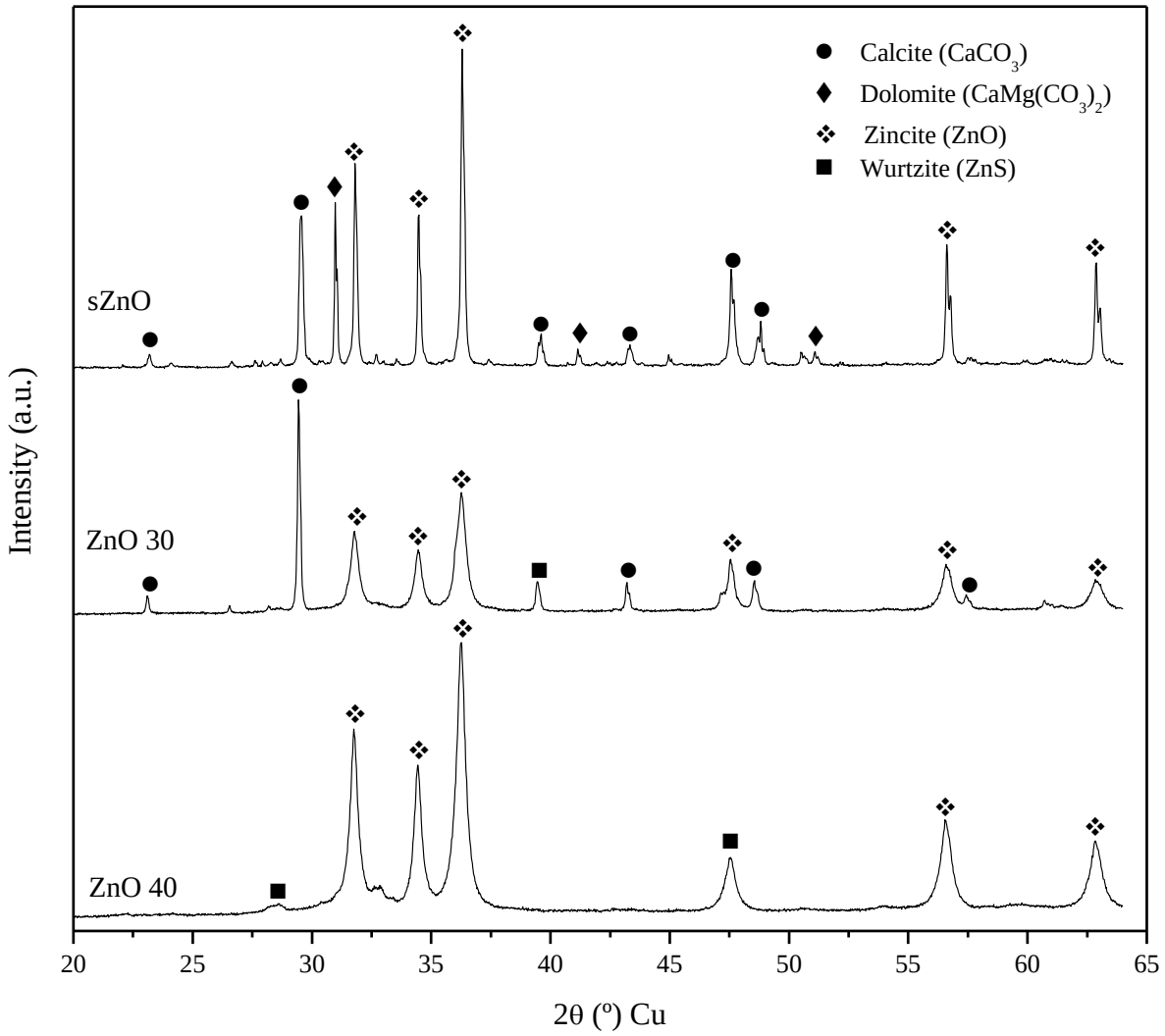
Calcite ($CaCO_3$)
Dolomite ($CaMg(CO_3)_2$)
Zincite (ZnO)
Wurtzite (ZnS)
sZnO
ZnO 30
ZnO 40
Intensity (a.u.)
20
25
30
35
40
45
50
55
60
65
2θ (º) Cu

Fig. 1.

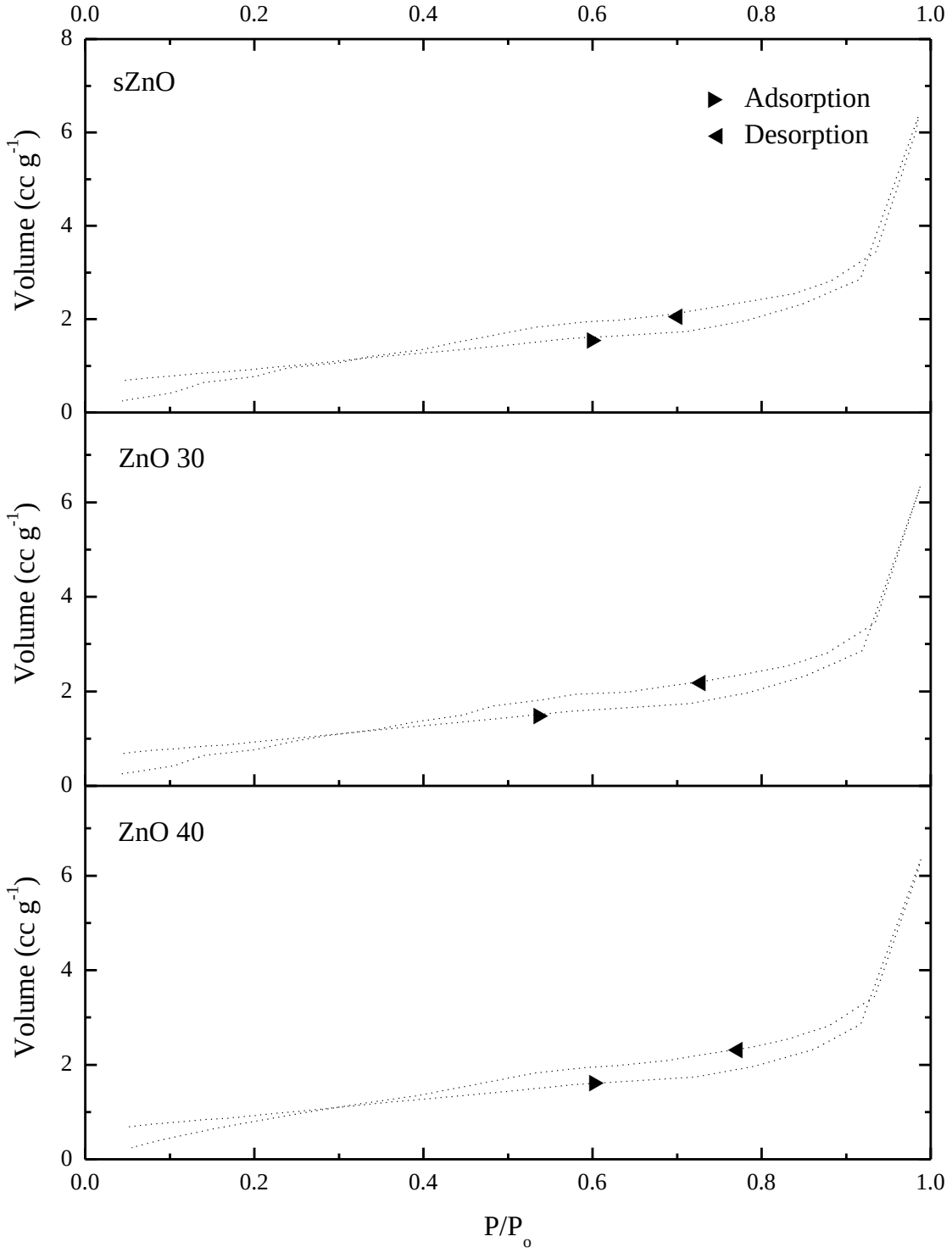
sZnO
Adsorption
Desorption
ZnO 30
ZnO 40
Volume (cc g-1)
P/Po
0.0
0.2
0.4
0.6
0.8
1.0
0
2
4
6
8

Fig. 2.

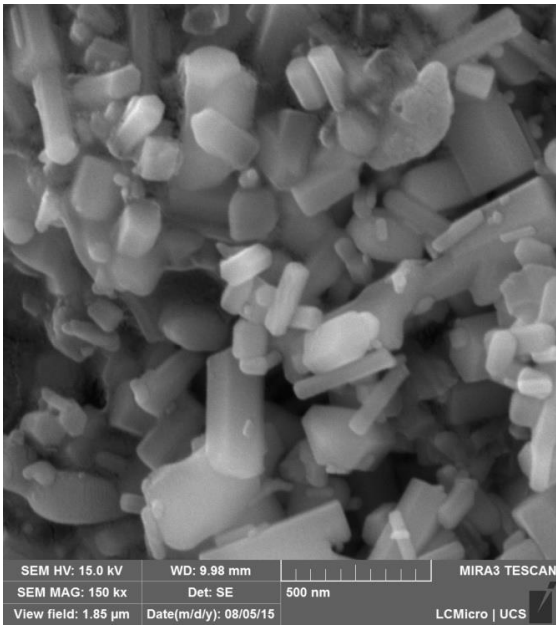
SEM HV: 15.0 kV
WD: 9.98 mm
MIRA3 TESCAN
SEM MAG: 150 kx
Det: SE
500 nm
View field: 1.85 µm
Date(m/d/y): 08/05/15
LCMicro | UCS

(a)

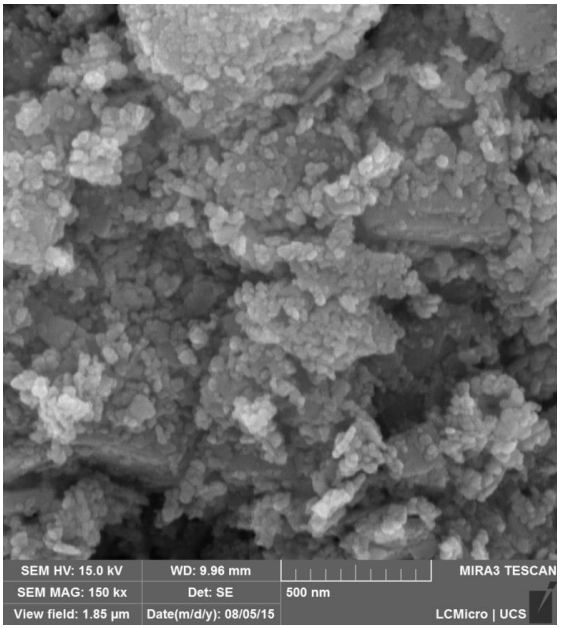
SEM HV: 15.0 kV
WD: 9.96 mm
MIRA3 TESCAN
SEM MAG: 150 kx
Det: SE
500 nm
View field: 1.85 µm
Date(m/d/y): 08/05/15
LCMicro | UCS

(b)

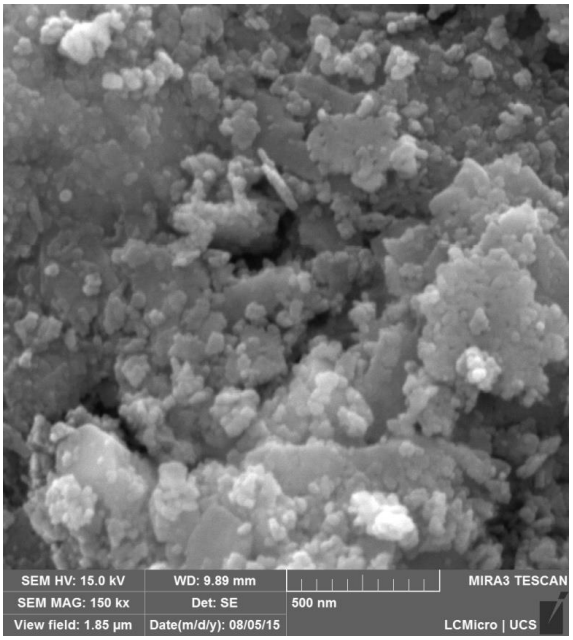
SEM HV: 15.0 kV
WD: 9.89 mm
MIRA3 TESCAN
SEM MAG: 150 kx
Det: SE
500 nm
View field: 1.85 µm
Date(m/d/y): 08/05/15
LCMicro | UCS

(c)

Fig. 3.

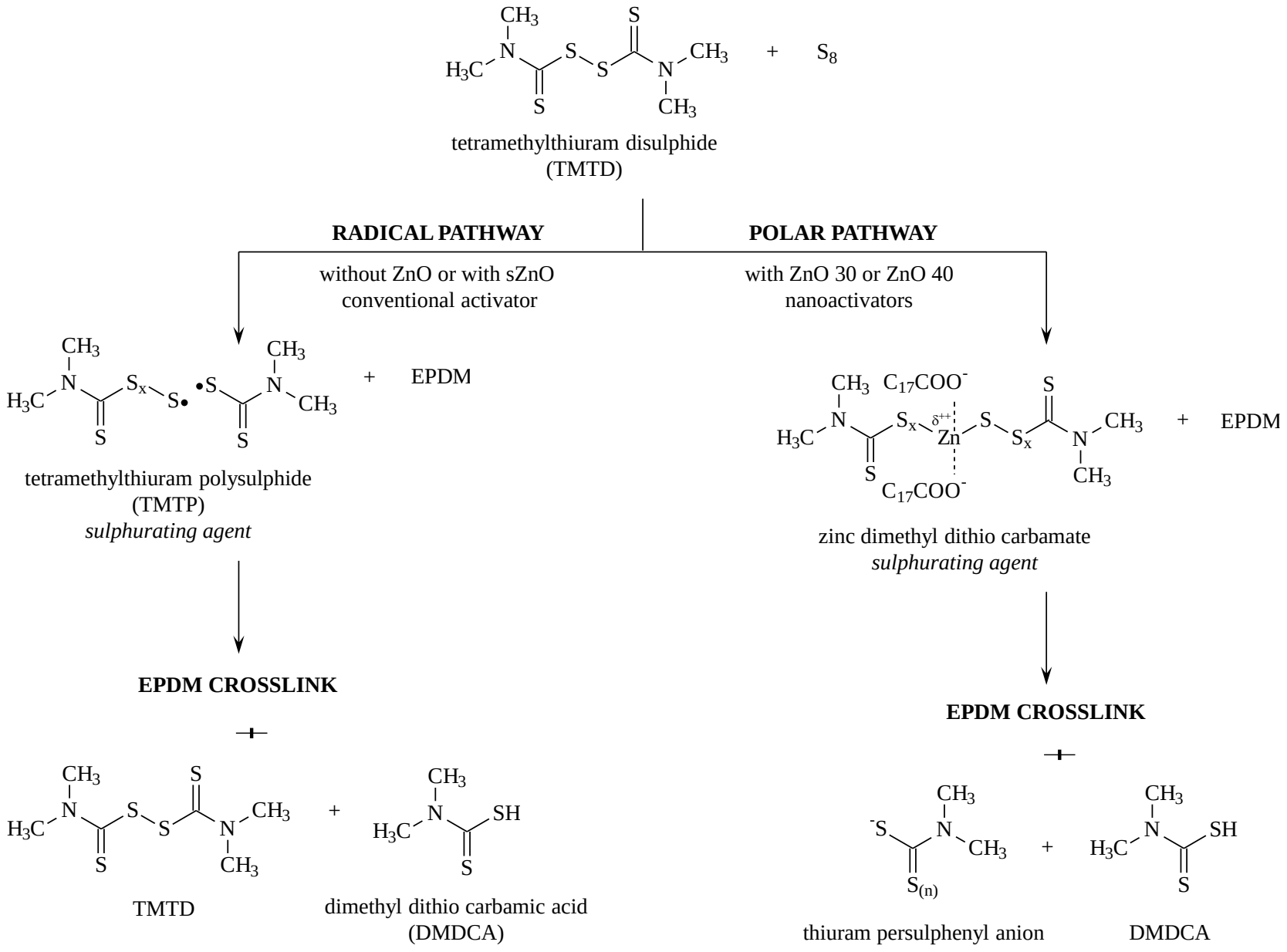
tetramethylthiuram disulphide
(TMTD)
RADICAL PATHWAY
POLAR PATHWAY
without ZnO or with sZnO
conventional activator
with ZnO 30 or ZnO 40
nanoactivators
tetramethylthiuram polysulphide
(TMTP)
sulphurating agent
EPDM
zinc dimethyl dithio carbamate
sulphurating agent
EPDM
EPDM CROSSLINK
EPDM CROSSLINK
TMTD
dimethyl dithio carbamic acid
(DMDCA)
thiuram persulphenyl anion
DMDCA

Fig. 4

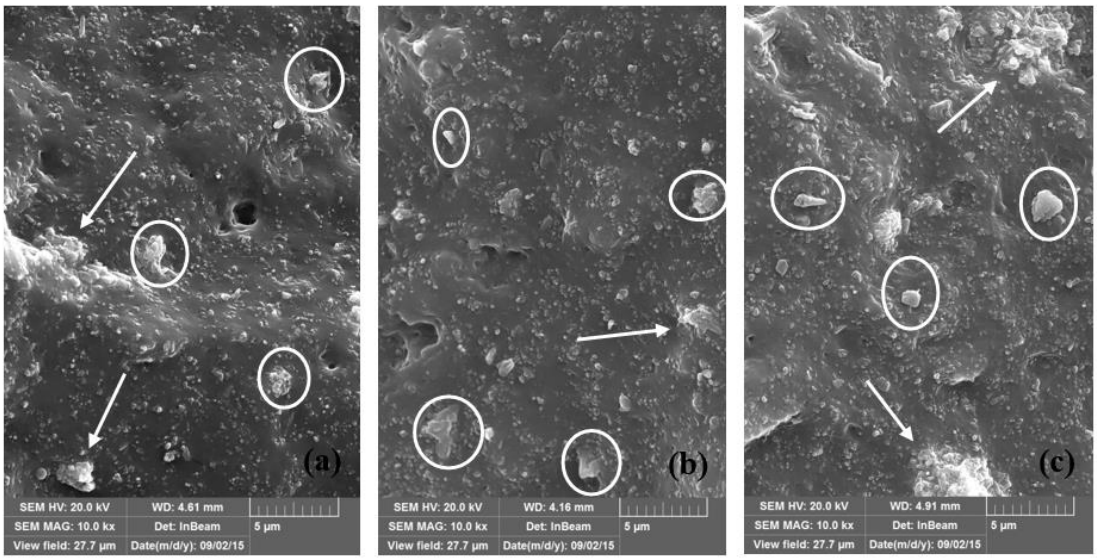
(a)
SEM HV: 20.0 kV
WD: 4.61 mm
SEM MAG: 10.0 kx
Det: InBeam
5 µm
View field: 27.7 µm
Date(m/d/y): 09/02/15
(b)
SEM HV: 20.0 kV
WD: 4.16 mm
SEM MAG: 10.0 kx
Det: InBeam
5 µm
View field: 27.7 µm
Date(m/d/y): 09/02/15
(c)
SEM HV: 20.0 kV
WD: 4.91 mm
SEM MAG: 10.0 kx
Det: InBeam
5 µm
View field: 27.7 µm
Date(m/d/y): 09/02/15

Fig. 5

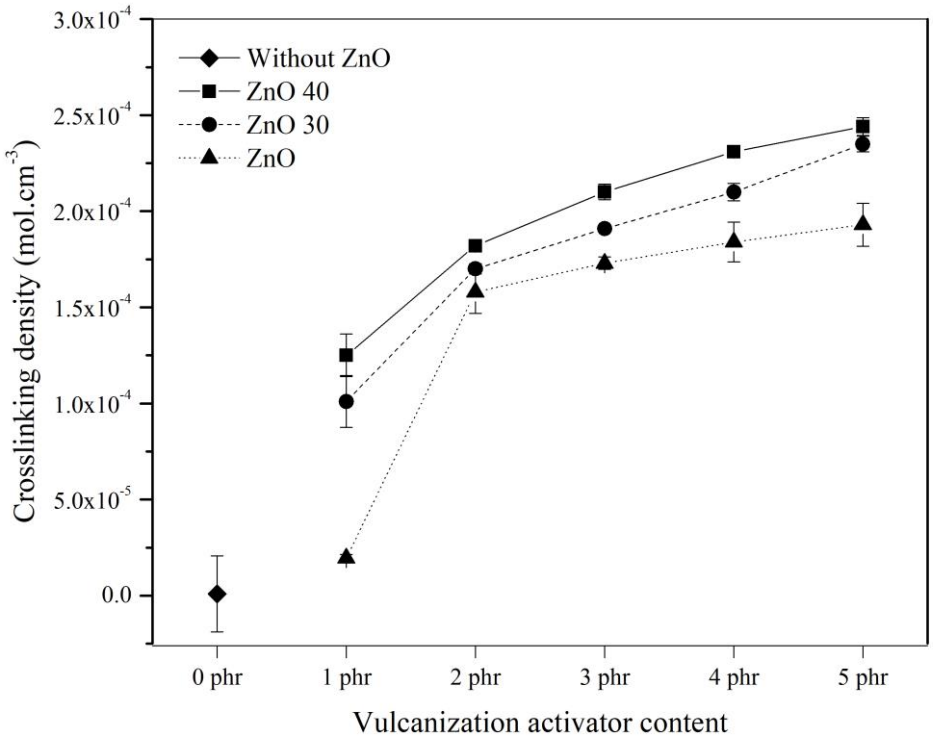
Without ZnO
ZnO 40
ZnO 30
ZnO
Crosslinking density (mol.cm-3)
3.0x10-4
2.5x10-4
2.0x10-4
1.5x10-4
1.0x10-4
5.0x10-5
0.0
0 phr
1 phr
2 phr
3 phr
4 phr
5 phr
Vulcanization activator content

Fig. 6

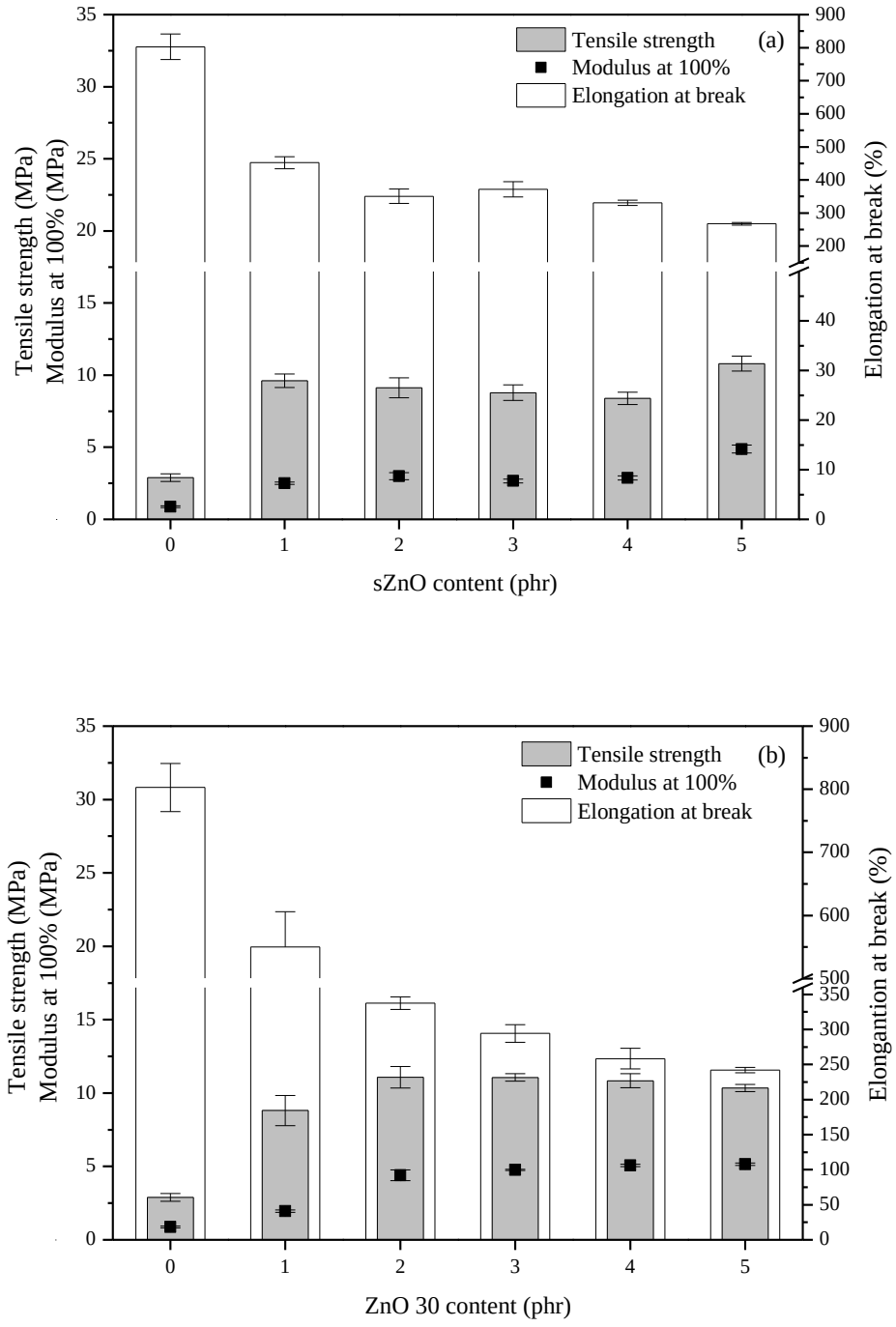
Tensile strength
Modulus at 100%
Elongation at break
(a)
Tensile strength (MPa)
Modulus at 100% (MPa)
Elongation at break (%)
sZnO content (phr)
(b)
Elongantion at break (%)
ZnO 30 content (phr)

Fig. 7

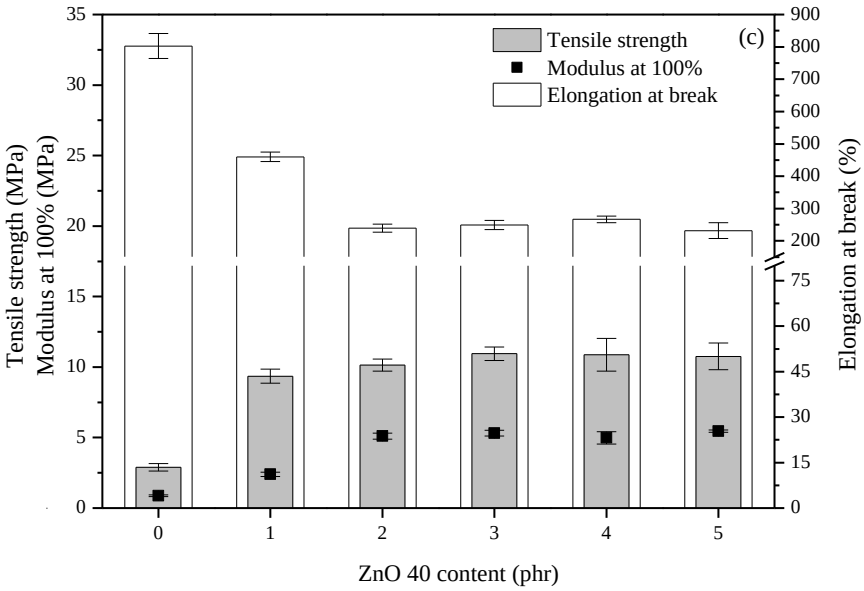

Fig. 7 (continuation)

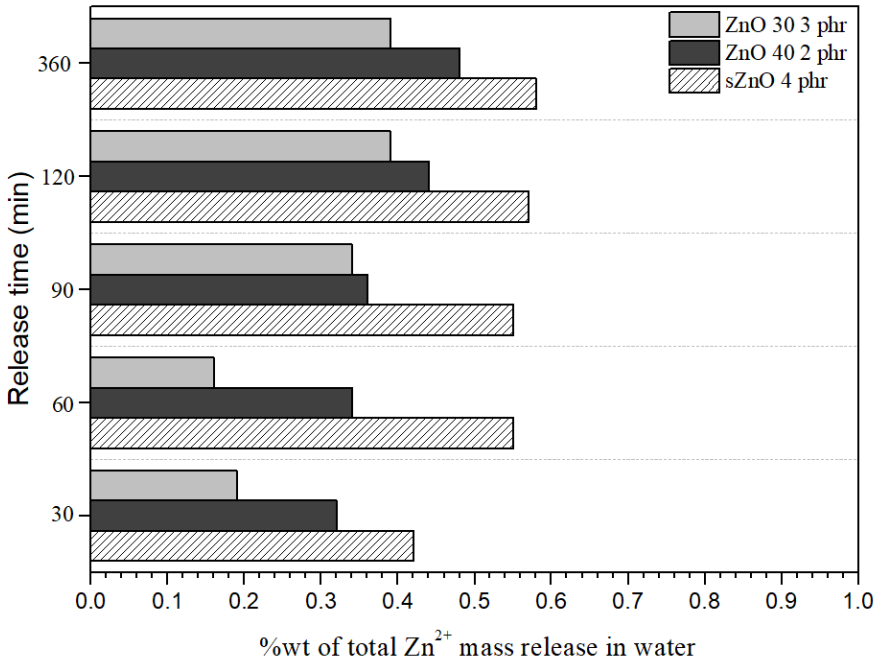

Fig. 8

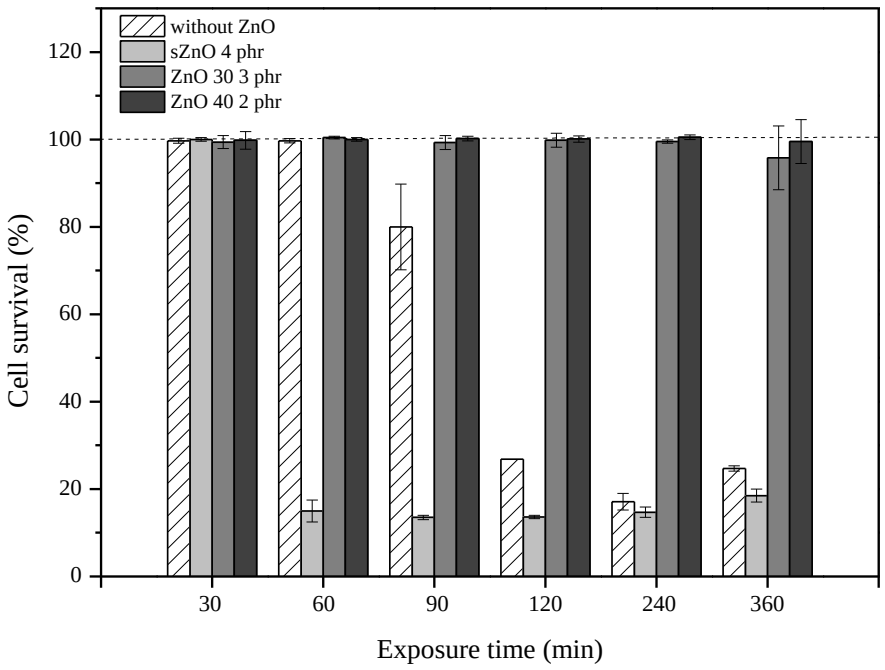
without ZnO
sZnO 4 phr
ZnO 30 3 phr
ZnO 40 2 phr
Cell survival (%)
0
20
40
60
80
100
120
30
60
90
120
240
360
Exposure time (min)

Fig. 9

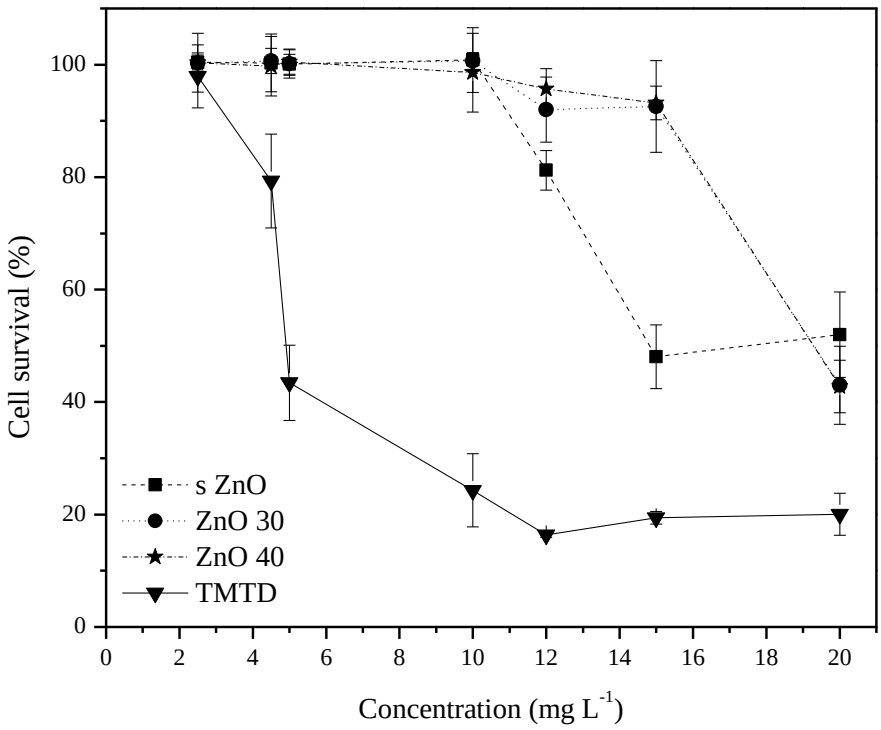
Cell survival (%)
Concentration (mg L-1)
s ZnO
ZnO 30
ZnO 40
TMTD
0
20
40
60
80
100
0
2
4
6
8
10
12
14
16
18
20

Fig. 10

Table 1. Surface area, total pore volumes and pore diameters of the ZnO, ZnO 30 and ZnO 40 samples.

Samples	Surface area (m^2g^{-1})[a]	V_{pore} (cm^3g^{-1})[b]	d_{pore}(nm)[c]
sZnO	3.44	0.009	3.2
ZnO 30	16.23	0.071	3.7
ZnO 40	23.85	0.084	3.6

[a]Determined from nitrogen gas adsorption-desorption isotherms using BET equation.
[b]Determined from cumulative adsorption pore volume using BJH method.
[c]Determined from adsorption pore size using BJH method.

Table 2. Viscosity Mooney of the elastomeric compositions with sZnO, ZnO 30 and ZnO 40.

ZnO content (phr)	Mooney Viscosity (ML (1+4) 100ºC)		
	sZnO	ZnO 30	ZnO 40
0	48.3 ± 1.0	-	-
1	47.6 ± 1.0	46.5 ± 1.0	46.4 ± 1.0
2	47.7 ± 1.0	61.0 ± 1.0	61.7 ± 1.0
3	47.7 ± 1.0	62.0 ± 1.0	61.9 ± 1.0
4	47.6 ± 1.0	60.8 ± 1.0	61.6 ± 1.0
5	61.6 ± 1.0	61.4 ± 1.0	60.3 ± 1.0

Table 3. Curing characteristics of the elastomeric compositions with sZnO, ZnO 30 and ZnO 40.

Sample	ZnO (phr)	M_L[a] (dNm)	M_H[b] (dNm)	ΔM (dNm)	t_{s1}[c] (min)	t_{90}[d] (min)	CRI[e] (min^{-1})
-	0	0.77	6.61	5.84	2.50	4.47	50.76
sZnO	1	0.71	19.56	18.78	2.16	10.91	11.43
	2	0.72	23.87	23.15	2.11	8.40	15.89
	3	0.73	24.50	23.77	2.13	7.61	18.24
	4	0.73	25.55	24.82	2.05	6.38	23.09
	5	1.00	28.93	27.93	1.71	5.86	24.09
ZnO 30	1	0.78	21.87	21.16	1.58	3.96	29.24
	2	0.91	26.09	25.18	1.56	4.41	35.08
	3	0.96	27.55	26.59	1.58	4.73	31.75
	4	0.92	29.78	28.86	1.50	5.33	26.11
	5	0.97	29.75	28.78	1.58	5.58	25.00
ZnO 40	1	0.75	22.30	21.56	1.50	4.60	32.25
	2	0.97	28.69	27.72	1.53	4.95	29.24
	3	0.97	32.00	31.03	1.55	5.36	26.25
	4	0.98	30.52	29.54	1.56	5.73	23.98
	5	0.93	30.16	29.23	1.55	5.73	23.81

[a]Minimum torque,[b]maximum torque,[c]scorch time,[d]optimal cure time,[e]cure rate index.

Table 4. Hardness and tear strength of the elastomeric compositionswith sZnO, ZnO 30 and ZnO 40.

Compositions	ZnO (phr)	Hardness (Shore A)	Tear Strength ($kNmin^{-1}$)
Without ZnO	0	48.7 ± 0.6	21.95 ± 2.40
sZnO	1	66.4 ± 0.4	25.49 ± 1.17
	2	67.6 ± 0.5	23.14 ± 1.97
	3	68.5 ± 0.5	22.70 ± 1.54
	4	68.6 ± 0.3	20.84 ± 0.51
	5	74.5 ± 0.2	20.66 ± 1.23
ZnO 30	1	61.7 ± 0.5	28.48 ± 1.12
	2	71.1 ± 0.4	26.04 ± 0.76
	3	74.5 ± 0.2	24.50 ± 0.97
	4	74.8 ± 0.3	22.92 ± 1.33
	5	75.1 ± 0.3	21.88 ± 1.02
ZnO 40	1	65.0 ± 0.6	26.28 ± 1.84
	2	74.1 ± 0.8	24.21 ± 0.33
	3	75.2 ± 0.3	22.34 ± 0.93
	4	74.7 ± 0.3	21.22 ± 1.73
	5	74.0 ± 0.6	20.28 ± 1.19